

## Hydrothermal Synthesis, Structure, and Magnetic Properties of the Mixed-Valent Np(IV)/Np(V) Selenite Np(NpO<sub>2</sub>)<sub>2</sub>(SeO<sub>3</sub>)<sub>3</sub>

Philip M. Almond,<sup>†</sup> Richard E. Sykora,<sup>†</sup> S. Skanthakumar,<sup>‡</sup> L. Soderholm,<sup>‡</sup> and Thomas E. Albrecht-Schmitt<sup>\*†</sup>

Department of Chemistry and Leach Nuclear Science Center, Auburn University, Auburn, Alabama 36849, and Chemistry Division, Argonne National Laboratory, Argonne, Illinois 60439

Received October 27, 2003

The reaction of NpO<sub>2</sub> with SeO<sub>2</sub> in the presence of CsCl at 180 °C results in the formation of Np(NpO<sub>2</sub>)<sub>2</sub>(SeO<sub>3</sub>)<sub>3</sub> (**1**). The structure of **1** consists of three crystallographically unique Np centers with three different coordination environments in two different oxidation states. Np(1) is found in a neptunyl(V), O=Np=O<sup>+</sup>, unit that is further ligated in the equatorial plane by three chelating SeO<sub>3</sub><sup>2-</sup> anions to create a hexagonal bipyramidal NpO<sub>8</sub> unit. A second neptunyl(V) cation also occurs for Np(2); it is bound by four bridging selenite anions and by the oxo atom from the Np(1) neptunyl cation to form a pentagonal bipyramidal, NpO<sub>7</sub>, unit. The third neptunium center, Np(3), which contains Np(IV), is found in a distorted NpO<sub>8</sub> dodecahedron. Np(3) is bound by five bridging selenite anions and by three neptunyl units via cation–cation interactions. The NpO<sub>7</sub> pentagonal bipyramids and NpO<sub>8</sub> hexagonal bipyramids share both corners and edges. Both of these polyhedra share corners via cation–cation interactions with the NpO<sub>8</sub> dodecahedra creating a three-dimensional structure with small channels that house the stereochemically active lone pair of electrons on the selenite anions. Magnetic susceptibility data follow Curie–Weiss behavior over the entire temperature range measured (5 ≤ *T* ≤ 320 K). The effective moment,  $\mu_{\text{eff}} = 2.28 \mu_{\text{B}}$ , which represents an average over the three crystallographically inequivalent Np atoms, is within the expected range of values. There is no evidence of long-range ordering of the Np moments at temperatures down to 5 K, consistent with the negligible Weiss constant determined from fitting the susceptibility data. Crystallographic data: **1**, orthorhombic, space group *Pbca*, *a* = 10.6216(5), *b* = 11.9695(6), and *c* = 17.8084(8) Å and *Z* = 8 (*T* = 193 K).

### Introduction

The solid-state chemistry of neptunium is as rich or perhaps even richer than that of uranium owing to the formation of numerous solids with oxidation states from +III to +VII.<sup>1</sup> Examples of mixed-valent oxides are quite well-known from binary oxides, e.g. Np<sub>3</sub>O<sub>8</sub> and Np<sub>4</sub>O<sub>9</sub>.<sup>2</sup> The +V and +VI oxidation states of neptunium are both typically stabilized by the formation of approximately linear actinyl,

NpO<sub>2</sub><sup>*n*+</sup> (*n* = 1 or 2), cations that are bound by four to six additional atoms perpendicular to the actinyl axis to yield NpO<sub>6</sub> tetragonal bipyramids, NpO<sub>7</sub>, pentagonal bipyramids, and NpO<sub>8</sub> hexagonal bipyramids.<sup>1</sup> In addition to oxidation state differences, there are substantial bonding differences that occur between the AnO<sub>2</sub><sup>+</sup> and AnO<sub>2</sub><sup>2+</sup> cations. First, AnO<sub>2</sub><sup>+</sup> complexes are far more labile in solution than those containing AnO<sub>2</sub><sup>2+</sup> owing to the lower effective charge of the former cations.<sup>3</sup> Second, AnO<sub>2</sub><sup>+</sup> cations have the ability to form cation–cation interactions (CCI's) whereby the once terminal oxo atoms of the actinyl unit are used to bind neighboring actinyl cations.<sup>4</sup> These interactions were first recognized to occur in solution and have been characterized by a wide variety of spectroscopic techniques,<sup>4,5</sup> but they

\* To whom correspondence should be addressed. E-mail: albreth@auburn.edu.

<sup>†</sup> Auburn University.

<sup>‡</sup> Argonne National Laboratory.

(1) Fahey, J. A. Neptunium. In *The Chemistry of the Actinide Elements*, 2nd ed.; Katz, J. J., Seaborg, G. T., Morss, L. R., Eds.; Chapman and Hall: London, 1986; Chapter 6, pp 443–498.

(2) (a) Fahey, J. A.; Turcotte, R. P.; Chikalla, T. D. *J. Inorg. Nucl. Chem.* **1976**, *38*, 495. (b) Katz, J. J.; Gruen, D. M. *J. Am. Chem. Soc.* **1949**, *71*, 2106. (c) Collins, D. A.; Phillips, G. M. *J. Inorg. Nucl. Chem.* **1958**, *6*, 67.

(3) Choppin, G. R. *Radiochim. Acta* **1983**, *32*, 43.

(4) Sullivan, J. C.; Hindman, J. C.; Zielen, A. J. *J. Am. Chem. Soc.* **1961**, *83*, 3373.

are now known to also be a key component of the solid-state chemistry of Np(V).<sup>6</sup>

Cation–cation interactions in solid-state neptunium(V) compounds give rise to dimers such as in [Na<sub>4</sub>(NpO<sub>2</sub>)<sub>2</sub>-(C<sub>12</sub>O<sub>12</sub>)]·8H<sub>2</sub>O,<sup>7</sup> one-dimensional chains in Cs<sub>3</sub>[NpO<sub>2</sub>(SO<sub>4</sub>)<sub>2</sub>]·H<sub>2</sub>O<sup>8</sup> and K<sub>3</sub>NpO<sub>2</sub>(CrO<sub>4</sub>)<sub>2</sub>,<sup>9</sup> two-dimensional sheets (e.g. in (NpO<sub>2</sub>)<sub>2</sub>C<sub>2</sub>O<sub>4</sub>·6H<sub>2</sub>O,<sup>10</sup> NpO<sub>2</sub>(IO<sub>3</sub>),<sup>11</sup> and β-AgNpO<sub>2</sub>(SeO<sub>3</sub>),<sup>11</sup> and three-dimensional networks (e.g. in (NpO<sub>2</sub>)<sub>2</sub>SO<sub>4</sub>·H<sub>2</sub>O<sup>12</sup> and Na<sub>2</sub>[(NpO<sub>2</sub>)<sub>2</sub>(MoO<sub>4</sub>)<sub>2</sub>H<sub>2</sub>O]·H<sub>2</sub>O).<sup>13</sup> These interactions yield Np(V)···Np(V) distances that are typically between 3.5 and 4.0 Å, and because the Np centers are bridged by a diamagnetic oxygen atom, these compounds provide a remarkable opportunity for superexchange magnetic interactions to be observed. <sup>237</sup>Np Mossbauer spectroscopic measurements on a series of neptunium compounds with carboxylate type ligands and cation–cation interactions revealed substantial magnetic hyperfine splitting indicative of possible magnetic ordering.<sup>14</sup>

Unfortunately, few studies on the magnetic susceptibility of neptunium compounds containing CCI's have taken place. In fact, these can be limited to the examination of the magnetic properties of [Na<sub>4</sub>(NpO<sub>2</sub>)<sub>2</sub>(C<sub>12</sub>O<sub>12</sub>)]·8H<sub>2</sub>O,<sup>7</sup> NpO<sub>2</sub>-(O<sub>2</sub>CH)(H<sub>2</sub>O),<sup>15</sup> [(NpO<sub>2</sub>)<sub>2</sub>(O<sub>2</sub>C)<sub>2</sub>C<sub>6</sub>H<sub>4</sub>]·3H<sub>2</sub>O,<sup>16</sup> (NpO<sub>2</sub>)<sub>2</sub>C<sub>2</sub>O<sub>4</sub>·4H<sub>2</sub>O,<sup>17</sup> and [NH<sub>4</sub>][NpO<sub>2</sub>(O<sub>2</sub>CH)<sub>2</sub>].<sup>14c</sup> These compounds show unusual magnetic behavior for coordination compounds of actinides in that there are long-range magnetic interactions and ordering. The magnetic properties of [Na<sub>4</sub>(NpO<sub>2</sub>)<sub>2</sub>-(C<sub>12</sub>O<sub>12</sub>)]·8H<sub>2</sub>O are not yet fully understood, but some type

of magnetic transition, perhaps to an ordered state, occurs at 10 K.<sup>7</sup> NpO<sub>2</sub>(O<sub>2</sub>CH)(H<sub>2</sub>O) shows spontaneous ferromagnetic ordering below 12.3 K, the highest ferromagnetic ordering temperature observed for a coordination compound of Np(V).<sup>15</sup> The behavior of NpO<sub>2</sub>(O<sub>2</sub>CH)(H<sub>2</sub>O) has been interpreted on the basis of an Ising-type model with the magnetic moment heavily restricted to the O=Np=O axis.<sup>15</sup> The Np(V) phthalate, [(NpO<sub>2</sub>)<sub>2</sub>(O<sub>2</sub>C)<sub>2</sub>C<sub>6</sub>H<sub>4</sub>]·4H<sub>2</sub>O, has a remarkably complex magnetic structure at low temperature that has been interpreted as containing both ferromagnetic and antiferromagnetic components with metamagnetic behavior being observed in magnetization experiments.<sup>16</sup> The magnetic properties of (NpO<sub>2</sub>)<sub>2</sub>C<sub>2</sub>O<sub>4</sub>·4H<sub>2</sub>O have been the subject of some controversy and have been interpreted on the basis of both metamagnetic<sup>16</sup> and ferromagnetic behavior.<sup>17</sup> Magnetic ordering in [NH<sub>4</sub>][NpO<sub>2</sub>(O<sub>2</sub>CH)<sub>2</sub>] has not been observed down to 2 K.<sup>14c</sup> The development of new, well-defined phases containing CCI's provides for additional opportunities to explore the electronic structure of Np(V) compounds as well as an increased understanding of the solid-state chemistry of neptunium, which is certainly well from resolved.

Herein we report the results of a series of experiments that have resulted in the synthesis, structural elucidation, and determination of the magnetic properties of the mixed-valent Np(IV)/Np(V) selenite Np(NpO<sub>2</sub>)<sub>2</sub>(SeO<sub>3</sub>)<sub>3</sub> (**1**). Np(NpO<sub>2</sub>)<sub>2</sub>-(SeO<sub>3</sub>)<sub>3</sub> (**1**) is the first mixed-valent neptunium compound containing cation–cation interactions between Np(V) and Np(IV). It is further remarkable in that it forms a three-dimensional channel structure, an attribute not common to compounds containing actinyl cations.<sup>18</sup>

## Experimental Section

**Syntheses.** <sup>237</sup>NpO<sub>2</sub> (99.9%, Oak Ridge), SeO<sub>2</sub> (99.4%, Alfa Aesar), and CsCl (99.9%, Alfa-Aesar) were used as received. Distilled and Millipore-filtered water with a resistance of 18.2 MΩ·cm was used in all reactions. Reactions were run in Parr 4749 autoclaves with custom-made 10-mL PTFE liners. Semiquantitative SEM/EDX analyses were performed using a JEOL 840/Link Isis instrument.

**Caution!** <sup>237</sup>Np (*t*<sub>1/2</sub> = 2.14 × 10<sup>6</sup> y) represents a serious health risk owing to its α and γ emission and especially because of its decay to the short-lived isotope <sup>233</sup>Pa (*t*<sub>1/2</sub> = 27.0 d), which is a potent β and γ emitter. All studies were conducted in a laboratory dedicated to studies on transuranium elements using procedures previously described.<sup>11</sup>

**Np(NpO<sub>2</sub>)<sub>2</sub>(SeO<sub>3</sub>)<sub>3</sub> (**1**).** NpO<sub>2</sub> (10 mg, 0.037 mmol), SeO<sub>2</sub> (8.2 mg, 0.074 mmol), and CsCl (12.5 mg, 0.074 mmol) were loaded in a 10-mL PTFE-lined autoclave followed by the addition of 0.34 mL of water. The autoclave was sealed and placed in a preheated furnace for 3 d at 180 °C. The box furnace was cooled at 9 °C/h to 23 °C. The product consisted of a colorless solution over brown prisms of **1**. The crystals were generally small and had a maximum dimension of approximately 0.080 mm. The majority of the mother liquor was removed from the crystals, and additional water was added to keep the crystals under solution. A few crystals of **1** were selected using digital microscope for X-ray diffraction studies. These

- (5) (a) Sullivan, J. C. *J. Am. Chem. Soc.* **1962**, *84*, 4256. (b) Sullivan, J. C. *Inorg. Chem.* **1964**, *3*, 315. (c) Murmann, R. K.; Sullivan, J. C. *Inorg. Chem.* **1967**, *6*, 892. (d) Rykov, A. G.; Frolov, A. A. *Radiokhimiya* **1972**, *14*, 709. (e) Frolov, A. A.; Rykov, A. G. *Radiokhimiya* **1974**, *16*, 556. (f) Rykov, A. G.; Frolov, A. A. *Radiokhimiya* **1975**, *17*, 187. (g) Madic, C.; Guillaume, B.; Morisseau, J. C.; Moulin, J. P. *J. Inorg. Nucl. Chem.* **1979**, *41*, 1027. (h) Guillaume, B.; Begun, G. M.; Hahn, R. L. *Inorg. Chem.* **1982**, *21*, 1159. (i) Madic, C.; Begun, G. M.; Hobart, D. E.; Hahn, R. L. *Radiokhimiya* **1983**, *34*, 195. (j) Andreev, G. B.; Budantseva, N. A.; Antipin, M. Yu.; Krot, N. N. *Russ. J. Coord. Chem.* **2002**, *28*, 434. (k) Stoyer, N. J.; Hoffman, D. C.; Silva, R. J. *Radiokhimiya* **2000**, *88*, 279. (l) Guillaume, B.; Hahn, R. L.; Narten, A. H. *Inorg. Chem.* **1983**, *22*, 109.
- (6) Krot, N. N.; Suglobov, D. N. *Radiokhimiya* **1989**, *31*, 1.
- (7) Cousson, A.; Dabos, S.; Abazli, H.; Nectoux, F.; Pagès, M.; Choppin, G. *J. Less-Common Met.* **1984**, *99*, 233.
- (8) Grigor'ev, M. S.; Yanovskii, A. I.; Fedoseev, A. M.; Budantseva, N. A.; Struchkov, Y. T. *Radiokhimiya* **1991**, *33*, 17.
- (9) Grigor'ev, M. S.; Plotnikova, T. E.; Baturin, N. A.; Budantseva, N. A.; Fedoseev, A. M. *Radiokhimiya* **1996**, *38*, 136.
- (10) Grigor'ev, M. S.; Charushnikova, I. A.; Krot, N. N.; Yanovskii, A. I.; Struchkov, Y. T. *Zh. Neorg. Khim.* **1996**, *41*, 539.
- (11) Albrecht-Schmitt, T. E.; Almond, P. M.; Sykora, R. E. *Inorg. Chem.* **2003**, *42*, 3788.
- (12) Grigor'ev, M. S.; Baturin, N. A.; Budantseva, N. A.; Fedoseev, A. M. *Radiokhimiya* **1993**, *35*, 29.
- (13) Grigor'ev, M. S.; Baturin, N. A.; Fedoseev, A. M.; Budantseva, N. A. *Russ. J. Coord. Chem.* **1994**, *20*, 523.
- (14) Nectoux, F.; Abazli, H.; Jové, J.; Cousson, A.; Pagès, M.; Gasperin, M.; Choppin, G. *J. Less-Common Met.* **1984**, *97*, 1. (b) Saeki, M.; Nakada, M.; Nakamoto, T.; Masaki, N. M.; Yamashita, T. *J. Alloys Compd.* **1998**, *271*, 176. (c) Nakada, M.; Nakamoto, T.; Masaki, N. M.; Saeki, M.; Yamashita, T.; Krot, N. N. Conference Proceedings of ICAME'97. *Hyperfine Interact. (C)* **1998**, *3*, 129.
- (15) Nakamoto, T.; Nakada, M.; Nakamura, A.; Haga, Y.; Onuki, Y. *Solid State Commun.* **1999**, *109*, 77.
- (16) (a) Nakamoto, T.; Nakada, M.; Nakamura, A. *Solid State Commun.* **2001**, *119*, 523. (b) Nakamoto, T.; Nakada, M.; Nakamura, A. *J. Nucl. Sci. Technol.* **2002**, *3*, 102.
- (17) Jones, E. R., Jr.; Stone, J. A. *J. Chem. Phys.* **1972**, *56*, 1343.

- (18) Burns, P. C.; Miller, M. L.; Ewing, R. C. *Can. Mineral.* **1996**, *34*, 845.

**Table 1.** Crystallographic Data for  $\text{Np}(\text{NpO}_2)_2(\text{SeO}_3)_3$  (**1**)

formula	$\text{Np}(\text{NpO}_2)_2(\text{SeO}_3)_3$
fw	1155.88
color and habit	brown, prism
space group	<i>Pbca</i> (No. 61)
<i>a</i> (Å)	10.6216(5)
<i>b</i> (Å)	11.9695(6)
<i>c</i> (Å)	17.8084(8)
<i>V</i> (Å <sup>3</sup> )	2264.1(2)
<i>Z</i>	8
<i>T</i> (°C)	−80
$\lambda$ (Å)	0.710 73
max $2\theta$ (deg)	56.56
$\rho_{\text{calcd}}$ (g cm <sup>−3</sup> )	6.782
$\mu$ (Mo $K\alpha$ ) (cm <sup>−1</sup> )	370.49
$R(F)$ for $F_o^2 > 2\sigma(F_o^2)^a$	0.0291
$R_w(F_o^2)^b$	0.0632

$$^a R(F) = \sum ||F_o| - |F_c|| / \sum |F_o|. \quad ^b R_w(F_o^2) = [\sum [w(F_o^2 - F_c^2)^2] / \sum wF_o^4]^{1/2}.$$

crystals were transferred in their mother liquor into a pool of Krytox oil.

**Crystallographic Studies.** A single crystal of  $\text{Np}(\text{NpO}_2)_2(\text{SeO}_3)_3$  (**1**) was mounted on a glass fiber and aligned on a Bruker SMART APEX CCD X-ray diffractometer. Intensity measurements were performed using graphite-monochromated Mo  $K\alpha$  radiation from a sealed tube and monochromator. SMART (v 5.624) was used for preliminary determination of the cell constants and data collection control. The intensities of reflections of a sphere were collected by a combination of 3 sets of exposures (frames). Each set had a different  $\phi$  angle for the crystal, and each exposure covered a range of  $0.3^\circ$  in  $\omega$ . A total of 1800 frames were collected with an exposure time/frame of 60 s.

For **1** determination of integral intensities and global refinement were performed with the Bruker SAINT (v 6.02) software package using a narrow-frame integration algorithm. A face-indexed analytical absorption correction was initially applied using XPREP, where individual shells of unmerged data were corrected analytically and exported in the same format.<sup>19</sup> These files were subsequently treated with a semiempirical absorption correction by SADABS.<sup>20</sup> The program suite SHELXTL (v 6.12) was used for space group determination (XPREP), direct methods structure solution (XS), and least-squares refinement (XL).<sup>19</sup> The final refinements included anisotropic displacement parameters for all atoms except O(7), which was refined isotropically because it was nonpositive definite, and a secondary extinction parameter. Some crystallographic details are given in Table 1. Additional details can be found in the Supporting Information.

**Magnetic Studies.** Magnetization measurements were conducted on 12.88 mg of polycrystalline  $\text{Np}(\text{NpO}_2)_2(\text{SeO}_3)_3$ , using a superconducting quantum interference device (SQUID) magnetometer, over the temperature range 5–320 K. Radiological hazards of <sup>237</sup>Np required double encapsulation of the sample in sealed aluminum holders that contributed significantly ( $\approx 80\%$ ) to the measured signal at the highest temperatures. Magnetization versus applied fields up to 25 000 G were measured at 10 K to check for linearity. The low total sample signal, coupled with the large contribution from the sample holder to the measured signal, required the application of a large applied field for adequate statistics. As a result, both zero-field-cooled (ZFC) and field-cooled (FC) susceptibility

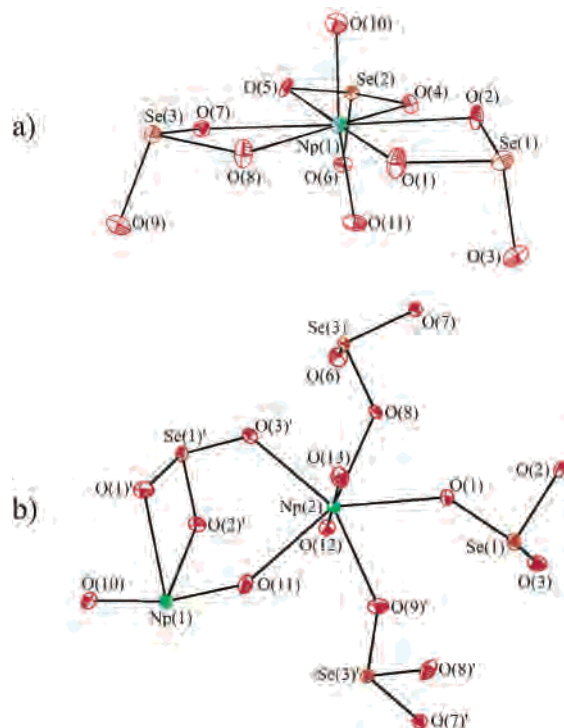


**Figure 1.** (a) Depiction of the  $\text{NpO}_3$  hexagonal bipyramidal environment for  $\text{Np}(1)$  formed from the chelation of a  $\text{NpO}_2^+$  cation by three  $\text{SeO}_3^{2-}$  anions in  $\text{Np}(\text{NpO}_2)_2(\text{SeO}_3)_3$  (**1**). (b) Illustration of the pentagonal bipyramidal geometry for  $\text{Np}(2)$  formed from the binding of a  $\text{NpO}_2^+$  cation by four bridging selenite anions and by the O(11) atom from the  $\text{Np}(1)$  neptunyl cation.

data were collected under an applied field of 2000 G. In addition, the low field magnetic response was measured at 20 and 50 G, as a function of temperature, to probe the samples for evidence of long-range magnetic ordering. The Al holders were measured separately under identical conditions, and their magnetic response was subtracted directly from the raw data. The diamagnetic response of the sample was calculated and added to the measured susceptibilities.

## Results and Discussion

**Synthesis.** The hydrothermal reaction of  $\text{NpO}_2$  with  $\text{SeO}_2$  in the presence of CsCl at 180 °C for 3 d results in the formation of  $\text{Np}(\text{NpO}_2)_2(\text{SeO}_3)_3$  (**1**) as small brown prisms. This product also forms in the presence other alkali metal chlorides. In the absence of a chloride source, no reaction is observed to take place between  $\text{NpO}_2$  with  $\text{SeO}_2$  under the aforementioned conditions. The chloride is apparently serving as a mineralizing agent and aids in dissolution of  $\text{NpO}_2$  and recrystallization of **1**.

**Structure of  $\text{Np}(\text{NpO}_2)_2(\text{SeO}_3)_3$  (**1**).** The structure of **1** is remarkable in that it consists of three crystallographically unique Np centers with three different coordination environments in two different oxidation states.  $\text{Np}(1)$  is found in a neptunyl unit with two short  $\text{Np}=\text{O}$  bonds of 1.861(6) and 1.883(7) Å. The neptunyl unit deviates strongly from linearity with a  $\text{O}(10)-\text{Np}(1)-\text{O}(11)$  bond angle of  $168.6(3)^\circ$ . The  $\text{Np}(1)$  center is further ligated in the equatorial plane by three chelating  $\text{SeO}_3^{2-}$  anions with  $\text{Np}-\text{O}$  bond distances ranging from 2.409(7) to 2.614(6) Å to create a hexagonal bipyramidal  $\text{NpO}_8$  unit as shown in Figure 1a. A second neptunyl

(19) Sheldrick, G. M. *SHELXTL PC, Version 6.12, An Integrated System for Solving, Refining, and Displaying Crystal Structures from Diffraction Data*; Siemens Analytical X-ray Instruments, Inc.: Madison, WI, 2001.

(20) Sheldrick, G. M. SADABS 2001, Program for absorption correction using SMART CCD based on the method of Blessing. Blessing, R. H. *Acta Crystallogr.* **1995**, *A51*, 33.

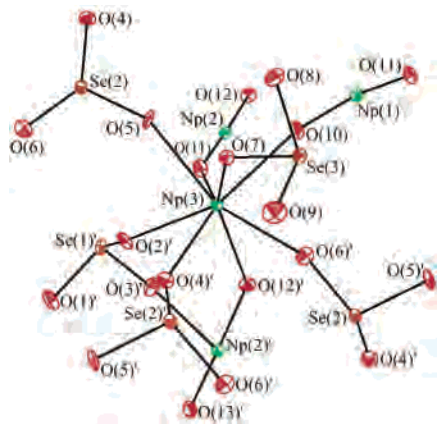


**Figure 2.** View of the distorted dodecahedral geometry around the Np(3) center in Np(NpO<sub>2</sub>)<sub>2</sub>(SeO<sub>3</sub>)<sub>3</sub> (1).

cation also occurs for Np(2) with two short Np=O bonds of 1.896(7) and 1.901(6) Å. As found for the neptunyl unit containing Np(1), the Np(2) neptunyl cation is also nonlinear with a O(12)–Np(2)–O(13) angle of 176.4(3)°. This cation is then bound by four bridging selenite anions and by the O(11) atom from the Np(1) neptunyl cation to form a pentagonal bipyramidal, NpO<sub>7</sub>, unit as depicted in Figure 1b. Therefore, there is a cation–cation, NpO<sub>2</sub><sup>+</sup>–NpO<sub>2</sub><sup>+</sup>, interaction between Np(1) and Np(2). The Np–O bond distances to the selenite anions range from 2.296(7) to 2.392(6) Å, whereas the Np(2)–O(11) distance of 2.514(7) Å is notably longer.

The final neptunium center, designated as Np(3), has a coordination environment completely different from that found for Np(1) or Np(2). Here Np is not found to occur in the form of a neptunyl unit but rather as a distorted NpO<sub>8</sub> dodecahedron,<sup>21</sup> as shown in Figure 2. Np(3) is bound by five bridging selenite anions and by three neptunyl units via cation–cation interactions. These cation–cation interactions occur with oxo atoms from the neptunyl units containing both Np(1) and Np(2). The Np–O distances to the selenite anions occur from 2.306(6) to 2.396(6) Å. The NpO<sub>2</sub><sup>+</sup>–Np(3) distances are in the same range as those that occur with the selenite anions and occur from 2.320(6) to 2.410(7) Å. The Se–O bond distances to the three crystallographically unique selenite anions are all within normal limits and occur from 1.649(7) to 1.752(7) Å. The Np···Np distances range from 3.9951(5) to 4.1758(5) Å.

Using Np(V)–O bond-valence parameters,<sup>11</sup> bond-valence sums were calculated for Np(1) and Np(2) to be 4.68 and 4.89, which are reasonably consistent with these sites containing Np(V).<sup>22</sup> The oxidation states of Np(1) and Np(2) can also be inferred from the Np=O bond distances which are notably longer than the Np(VI)=O bonds found in NpO<sub>2</sub>(IO<sub>3</sub>)<sub>2</sub>(H<sub>2</sub>O) and NpO<sub>2</sub>(IO<sub>3</sub>)<sub>2</sub>·H<sub>2</sub>O, which have an average distance of 1.763(8) Å.<sup>23</sup> Furthermore, the equatorial atoms in Np(VI) polyhedra are typically quite planar, whereas

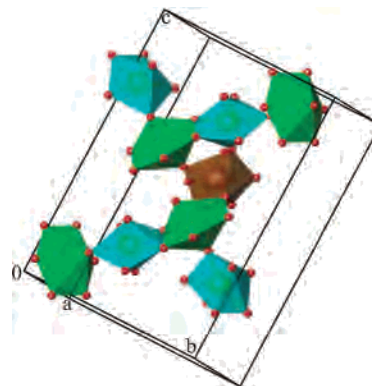


**Figure 3.** Simplified polyhedral depiction of the network that is formed from NpO<sub>7</sub> pentagonal bipyramids and NpO<sub>8</sub> hexagonal bipyramids that share both corners and edges. The corner-sharing occurs via the cation–cation interaction, and the edge-sharing, via μ<sub>3</sub>-oxo atoms from the selenite anions. Both of these polyhedra share corners via CCI's with the NpO<sub>8</sub> dodecahedra.

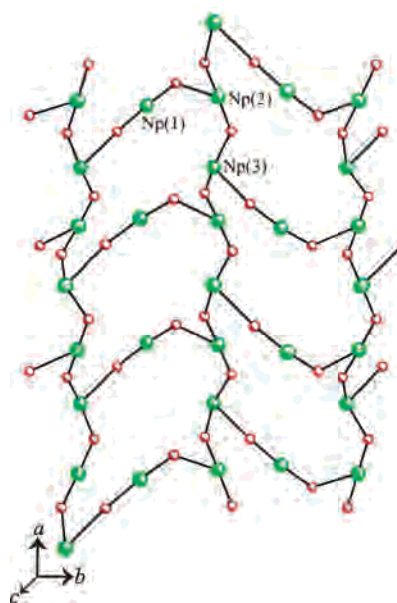


**Figure 4.** View of the two-dimensional network in the [ab] plane that is formed from the cation–cation interactions between the NpO<sub>7</sub> pentagonal bipyramids, NpO<sub>8</sub> hexagonal bipyramids, and NpO<sub>8</sub> dodecahedra.

those in Np(V) units can show substantial deviation from planarity. For Np(2), the equatorial oxygen atoms deviate from planarity by 0.59 Å. The bond-valence sum for Np(3) cannot currently be determined because the Np(IV)–O bond-valence parameter is unavailable, but using charge neutral requirements based on two NpO<sub>2</sub><sup>+</sup> cations and three SeO<sub>3</sub><sup>2-</sup> anions, one arrives at an oxidation state of IV for Np(3), which is consistent with its coordination environment.

The NpO<sub>7</sub> pentagonal bipyramids and NpO<sub>8</sub> hexagonal bipyramids share both corners and edges. The corner-sharing occurs via the cation–cation interaction, and the edge-sharing, via μ<sub>3</sub>-oxo atoms from the selenite anions. Both of these polyhedra share corners via CCI's with the NpO<sub>8</sub> dodecahedra. A simplified polyhedral depiction of the resultant network is shown in Figure 3. The cation–cation interactions between the Np(V) and Np(IV) units creates a puckered sheet that is shown in Figure 4. Two-dimensional networks formed from CCI's in neptunyl(V) compounds have

(21) Penneman, R. A.; Ryan, R. R.; Rosenzweig, A. *Struct. Bonding* **1973**, *13*, 1.

(22) (a) Brown, I. D.; Altermatt, D. *Acta Crystallogr.* **1985**, *B41*, 244. (b) Brese, N. E.; O'Keeffe, M. *Acta Crystallogr.* **1991**, *B47*, 192.

(23) Bean, A. C.; Scott, B. L.; Albrecht-Schmitt, T. E.; Runde, W. *Inorg. Chem.* **2003**, *42*, 5632.

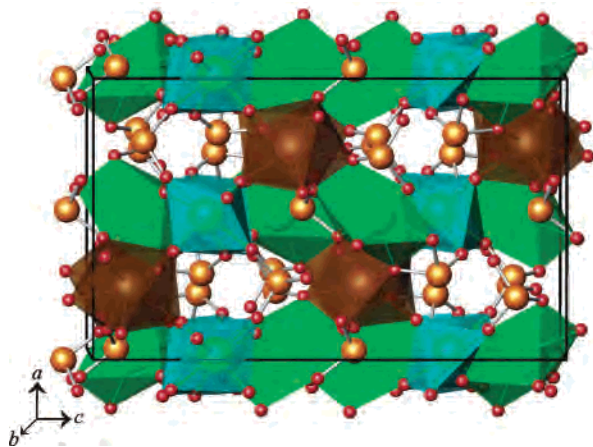


**Figure 5.** Complete polyhedral depiction of the complex unit cell for  $\text{Np}(\text{NpO}_2)_2(\text{SeO}_3)_3$  (**1**).

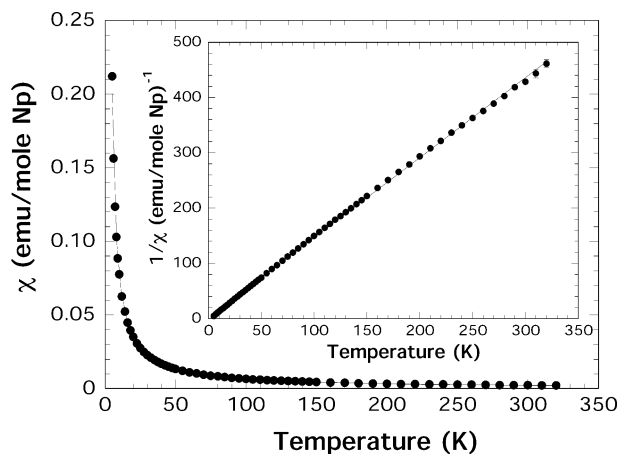


**Figure 6.** Magnetic susceptibility of  $\text{Np}(\text{NpO}_2)_2(\text{SeO}_3)_3$ , plotted as a function of temperature. The data, obtained under an applied field of 2000 G, were corrected for their diamagnetic contribution. The inset shows the same data as a Curie–Weiss plot, which shows linear behavior consistent with minimal contributions from  $\chi_{\text{TIP}}$  and crystal-field effects. The lines through the data represent the fit as discussed in the text.

been previously observed.<sup>10,11</sup> However, this network is substantially different owing to the presence  $\text{Np}(\text{IV})$ . In fact, this compound provides the first evidence for CCI's between  $\text{Np}(\text{IV})$  and  $\text{Np}(\text{V})$ . A complete polyhedral depiction of the complex unit cell for **1** is shown in Figure 5. It can be noted from this latter figure that channels are created in the structure that run down the  $b$  axis. These channels house the stereochemically active lone pair of electrons on the selenite anions; similar channels also occur in  $\beta\text{-AgNpO}_2\text{-}(\text{SeO}_3)$ .<sup>11</sup>

**Magnetic Properties.** The magnetization of  $\text{Np}(\text{NpO}_2)_2\text{-}(\text{SeO}_3)_3$ , obtained as a function of applied field at 10 K, is linear up to the highest measured field, 2.5 T. The magnetic susceptibility data, measured as a function of temperature under an applied field of 2000 G, are shown in Figure 6. The susceptibility decreases smoothly with increasing temperature. The absence of a cusp or discontinuity in the susceptibility is confirmed with low-field measurements that show similar behavior and also no significant difference between data obtained from FC and ZFC measurements. Taken together, there is no evidence of either long-range or spin-glass ordering of Np moments at temperatures as low

as 5 K. Instead, the Np spins behave as independent, isolated moments. The susceptibility data were least-squares fit to  $\chi(T) = C/(T + \Theta) + \chi_0$ , where  $C$  is the Curie constant,  $\Theta$  is the Weiss constant, and  $\chi_0$  is the temperature-independent susceptibility.<sup>24</sup> The refined parameters corresponding to the best fit of the data in the temperature range 5–320 K are  $C = 0.638$  K,  $\Theta = -2(2)$  K, and  $\chi_0 = 0.000\ 20(2)$ . The measured effective moment is derived from the Curie constant by following  $\mu_{\text{eff}} = [(3kC)/N]^{1/2}$ , where  $N$  is Avogadro's number, and is found to be  $\mu_{\text{eff}} = 2.26(8) \mu_{\text{B}}$ . The small value of the Weiss constant is consistent with single-ion magnetic properties with no evidence of magnetic ordering. The small temperature-independent susceptibility indicates that the Np moments are localized and not itinerant. This fit to the data is visually confirmed by the Curie–Weiss plot shown as an inset in Figure 6. The inverse susceptibility data as a function of temperature are linear, showing evidence of neither a significant temperature-independent susceptibility nor low-lying crystal field states. The linear fit to these data, which is sensitive to the higher temperature component, results in an effective moment  $\mu_{\text{eff}} = 2.30(5) \mu_{\text{B}}$  and  $\Theta = 1.1(20)$  K.

The measured effective moment reflects an average contribution to the susceptibility of three crystallographically inequivalent neptunium atoms,  $\text{Np}(1)$  and  $\text{Np}(2)$ , both of which are formally pentavalent, and  $\text{Np}(3)$ , which is formally tetravalent. Free-ion effective moments  $\mu_{\text{eff}}^{\text{FI}} = g[J(J + 1)]^{1/2} \mu_{\text{B}}$  can be calculated, using Russell–Saunders coupling, for  $\text{Np}(\text{V})$  of  $3.58 \mu_{\text{B}}$  and  $\text{Np}(\text{IV})$  of  $3.62 \mu_{\text{B}}$ .<sup>25</sup> If one averages the contributions from the different sites, the free-ion effective moment expected for this sample is  $3.59 \mu_{\text{B}}$ , which is significantly larger than that measured experimentally. The observation of an effective moment that is reduced from the free-ion value is not surprising because the ground term is split by a large crystal-field component in  $5f$  systems. The overall splitting can be on the order of 600 K.<sup>26</sup> This splitting can significantly reduce the measured susceptibility. For example, in a cubic environment the free-ion term of  $\text{Np}(\text{V})$  can be split such that the  $\Gamma_5$  triplet is isolated as the ground state, with an effective moment of  $2.8 \mu_{\text{B}}$ . The splitting can be sufficient to render the measured susceptibility linear over the temperature range under study here. Similarly,  $\text{Np}(\text{IV})$  in a cubic crystal field of appropriate symmetry can have a moment ranging from 1.3 to  $3.10 \mu_{\text{B}}$ . Although there is insufficient data to yield detailed electronic information about the Np paramagnetism exhibited by  $\text{Np}(\text{NpO}_2)_2(\text{SeO}_3)_3$ , it is clear that the observed susceptibility is consistent with known single ion magnetic responses of  $\text{Np}(\text{V})$  and  $\text{Np}(\text{IV})$  systems.

There is no evidence of magnetic ordering of the Np moments down to the lowest temperature studied. There have been several published reports of  $\text{Np}(\text{V})$ <sup>7,14c,15–17,27</sup> and

(24) Orchard, A. F. *Magnetochemistry*; Oxford University Press: Oxford, U.K., 2003; p 172.

(25) White, R. M. *Quantum Theory of Magnetism*, 2nd ed.; Springer-Verlag: Berlin, 1983; p 282.

(26) Amoretti, G.; Baise, A.; Boge, M.; Bonnisseau, D.; Burlet, P.; Collard, J. M.; Fournier, J. M.; Quezel, S.; Rossat-Mignod, J. *J. Magn. Magn. Mater.* **1989**, *79*, 207.

**Table 2.** Selected Bond Distances (Å) and Angles (deg) for Np(NpO<sub>2</sub>)<sub>2</sub>(SeO<sub>3</sub>)<sub>3</sub> (**1**)

Distances			
Np(1)–O(1)	2.409(7)	Np(3)–O(4)	2.326(6)
Np(1)–O(2)	2.432(6)	Np(3)–O(5)	2.360(6)
Np(1)–O(4)	2.529(6)	Np(3)–O(6)	2.396(6)
Np(1)–O(5)	2.614(6)	Np(3)–O(7)	2.306(6)
Np(1)–O(7)	2.523(6)	Np(3)–O(10)	2.355(6)
Np(1)–O(8)	2.424(6)	Np(3)–O(12)	2.320(6)
Np(1)–O(10)	1.883(7) (NpO <sub>2</sub> <sup>+</sup> )	Np(3)–O(13)	2.410(7)
Np(1)–O(11)	1.861(6) (NpO <sub>2</sub> <sup>+</sup> )	Se(1)–O(1)	1.722(7)
Np(2)–O(1)	2.392(6)	Se(1)–O(2)	1.752(7)
Np(2)–O(3)	2.362(7)	Se(1)–O(3)	1.649(7)
Np(2)–O(8)	2.335(6)	Se(2)–O(4)	1.738(6)
Np(2)–O(9)	2.296(7)	Se(2)–O(5)	1.710(6)
Np(2)–O(11)	2.514(7)	Se(2)–O(6)	1.674(7)
Np(2)–O(12)	1.901(6) (NpO <sub>2</sub> <sup>+</sup> )	Se(3)–O(7)	1.724(6)
Np(2)–O(13)	1.896(7) (NpO <sub>2</sub> <sup>+</sup> )	Se(3)–O(8)	1.716(6)
Np(3)–O(2)	2.371(6)	Se(3)–O(9)	1.660(7)
Np(1)–Np(2)	4.0327(5)	Np(1)–Np(3)	4.0877(5)
Np(1)–Np(2)	4.0411(5)	Np(1)–Np(3)	4.1590(5)
Np(1)–Np(3)	4.0506(5)	Np(2)–Np(3)	3.9951(5)
Np(2)–Np(3)	4.1758(5)		
Angles			
O(10)–Np(1)–O(11)	168.6(3)	O(12)–Np(2)–O(13)	176.4(3)

Np(IV)<sup>28–30</sup> compounds in which Np, coupled through oxygen superexchange pathways, order at low temperature. There is no report of ordering in a Np(V)/Np(IV) mixed-valent system. The onset temperature of long-range magnetic ordering is dependent upon the symmetry of the ground state, the magnitude of the magnetic moment, the metal–metal distance, and the symmetry and dimensionality of the crystal

lattice. Unfortunately, little direct evidence is available about the electronic and magnetic properties of the three crystallographically independent Np to comment on the ground-state moment. The two-dimensional Np(IV)–Np(V) network shown in Figure 4 has metal distances and connectivity that are consistent with previous systems that have been reported to show cooperative ordering. The Np–Np distances, listed in Table 2, are relatively short compared to Np compounds that have been previously reported to magnetically order.<sup>30</sup> In contrast, NpOSe, in which the Np(IV) moments order antiferromagnetically below 11 K, has short Np–Np bond distances of only 3.8042 and 3.8820 Å.<sup>26</sup>

**Acknowledgment.** This work was supported by the U.S. Department of Energy, Office of Basic Energy Sciences, Heavy Elements Program, under Grants DE-FG02-01ER15187 (Auburn University) and W-31-109-ENG-38 (Argonne National Laboratory).

**Supporting Information Available:** X-ray crystallographic files for Np(NpO<sub>2</sub>)<sub>2</sub>(SeO<sub>3</sub>)<sub>3</sub> (**1**) in CIF format. This material is available free of charge via the Internet at <http://pubs.acs.org>.

IC035241X

- (27) Nakamoto, T.; Nakada, M.; Nakamura, A. *Recent Res. Dev. Inorg. Chem.* **2000**, *2*, 145.
- (28) Caciuffo, R.; Paixao, J. A.; Detlefs, C.; Longfield, M. J.; Santini, P.; Bernhoeft, N.; Rebizant, J.; Lander, G. H. *J. Phys.: Condens. Matter* **2003**, *15*, S2287.
- (29) Lovesey, S. W.; Balcar, E.; Detlefs, C.; van der Laan, G.; Sivia, D. S.; Staub, U. *J. Phys.: Condens. Matter* **2003**, *15*, 4511.
- (30) Bickel, M.; Kanellakopoulos, B. *J. Solid State Chem.* **1993**, *107*, 273.